Design & Simulation of a CMOS MEMS using Standard Microelectronic CAD Environment

L. Latorre, V. Beroulle, P. Nouet.

Laboratoire d'Informatique, de Robotique et de Microélectronique de Montpellier
161, rue Ada, 34392 Montpellier Cedex 5, latorre@lirmm.fr

ABSTRACT

This paper addresses the design of CMOS monolithic microsystems through a case study. An increasing interest is given to such devices, which are intended to address large volume markets where batch fabrication is the only solution. This work demonstrates the efficiency of standard microelectronic CAD tools for MEMS design and simulation. The proposed design example is based on the super-heterodyne spectrum analyzer using a mechanical structure to achieve the high-Q filtering.

Keywords: CMOS MEMS, Mechanical filtering, Spectral Analysis, Spectre-RF®.

1 INTRODUCTION

The world of micro electro-mechanical systems includes several design and fabrication approaches. Motivated by the communication market, which is harshly ruled by cost and size of the components, the monolithic co-integration of MEMS together with standard microelectronics appears to be more than ever an obvious objective [1]. In this context, a lot of work is done to make MEMS compatible with standard technologies. This compatibility applies for both fabrication and design methodologies.

For complex circuits, it is common start describing the system using a high-level model. When progressing in such a top-down design methodology, the functional blocks are described using various representations (i.e. behavioral, gate level, transistor level...). At each step of the design process, system level simulations are performed to check for the initial specifications.

This paper deals with the design of a multi-physic integrated system in a standard microelectronic environment. Part two introduces the proposed system, which includes an electronic mixer and a mechanical high-Q filter in a spectral analysis application. Their integration in the standard design flow is discussed using both transistor level description and behavioral analog HDL. The third part develops the simulation approach, making use of recent advances in commercially available simulator engines. It finally presents the obtained results.

2 DESIGN EXAMPLE

The proposed example is based on the swept frequency, super-heterodyne spectrum analyzer [2], whose simplified block diagram is given figure 1. The signal V_{meas} to be analyzed is first multiplied by a frequency swept signal V_{fs}. The input signal is thus shifted in the frequency domain. Each time the frequency of the mixer output V_{mix} matches the band pass filter central frequency ω_0, an ac voltage peak occurs at the system output. Since both the filter characteristics and the frequency of V_{fs} are calibrated, the input signal spectrum is easily reconstructed.

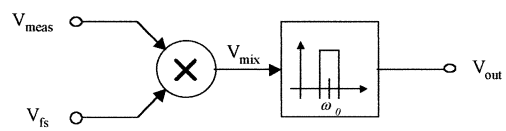

Figure 1: Simplified architecture for an analog spectrum analyzer

2.1 Mixer

A traditional Gilbert cell has been considered to implement the mixer. In the design software, this cell is described at the transistor level as shown on figure 2.

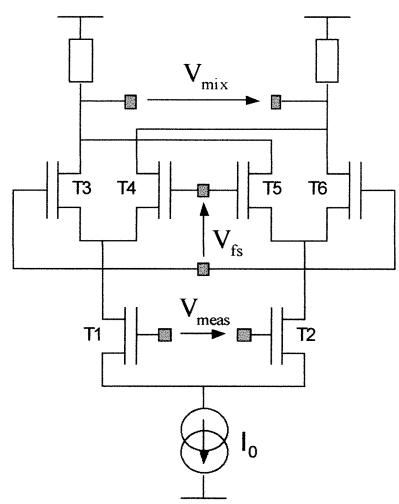

Figure 2: Transistor level description of the mixer.

This cell is based on a regular differential amplifier stage made of the transistors T1 and T2 in association with resistive loads. The mixing effect comes the four transmission gates T3 to T6 that are able to reverse the output polarity, thus switching the amplifier gain from A to –A depending on the voltage applied on the differential input V_{fs}. Although not a real analog multiplier, such mixer actually performs the required frequency shift but also add undesired sidebands due to the digital nature (square wave) of the switching command.

2.2 Mechanical filter

In order to increase the frequency resolution of the analyzer, a high-Q CMOS mechanical resonator implements the filter. This electromechanical filter is shown on figure 3. The input voltage is applied across a current path. In combination with an external dc magnetic field, it produces a Lorentz force that deforms the beam. The output voltage is then taken from a resistor bridge including a polysilicon strain gauge located on the suspended structure. For this application, the external magnetic field can be applied by means of a permanent magnet attached to the device package.

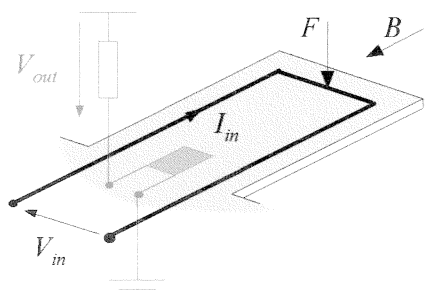

Figure 3: Principle of the mechanical filter.

Physical modeling of such cantilever has been extensively studied and reported [3]. The frequency response of such beams is well represented by a second order system transfer function:

$$\frac{V_{out}}{V_{in}} = \frac{S_{stat}}{1 + 2 \cdot \xi \frac{p}{\omega_0} + \frac{p^2}{\omega_0^2}} \qquad (1)$$

Where S_{stat} represents the static gain, including the beam response to the force, the electro-mechanical conversion of the gauge and the resistor bridge response. Due to the extremely small damping coefficient ξ obtained with such mechanical devices, the second-order low-pass filter exhibits strong resonance phenomenon (figure 4) that is profitably used to implement band-pass filter.

The spectral analyzer performance in terms of frequency resolution strongly relies on the filter bandwidth $\Delta\omega$. This bandwidth depends on the beam quality factor Q as given by:

$$\Delta\omega = \frac{\omega_0}{Q} = 2\xi\omega_0 \qquad (2)$$

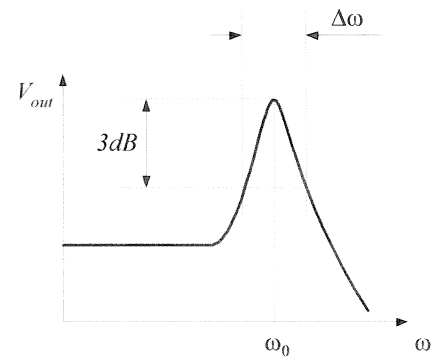

Figure 4: Typical frequency response of a low-damped second order mechanical system.

On fabricated test structures (figure 5), resonant frequencies have been measured around *9kHz*. The *-3dB* bandwidth around resonance is *150Hz* (*Q=60*) when operated in air. Under vacuum conditions the bandwidth drop down to *4Hz* (*Q=2250*) allowing for high-resolution spectrum analysis.

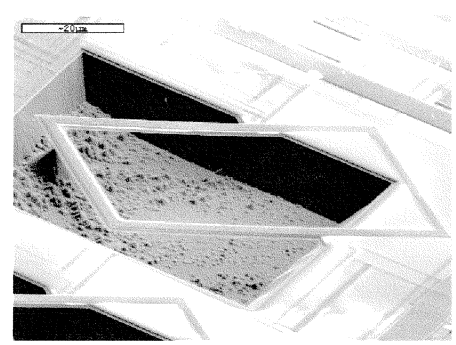

Figure 5: Example of fabricated cantilever filter.

The filter is finally integrated into the design flow by translating the model equations into a Verilog-A® module. This model is given figure 6. The filter interface is firstly stated: *fa* and *fb* are the electrical inputs for V_{in} and B is the magnetic field. *ra* and *rb* provide an access to the polysilicon gauge, whereas *z* represent the beam bending (in meters) and is used for debug purpose only. The next part of the model is used to set the various parameters to an initial value. Then comes the behavioral description. The magnetic force is calculated first using both input voltage and magnetic field data. Next, the second-order differential equation set is solved. Finally, the bending is translated into the gauge resistance variation. Note that both electrical and mechanical noise sources have been included in the filter description.

```
// Cantilever Module Definition

module Cantilever(fa, fb, B, ra, rb, z);

input  fa, fb;  electrical fa, fb;
input  B;       magnetic_2 B;
output ra, rb;  electrical ra, rb;
output z;       kinematic z;

// High-level Design Parameters
parameter real K  = 2.4;          // Spring constant
parameter real M  = 7.5e-10;      // Mass
parameter real D  = 7e-7;         // Damping factor
parameter real Lc = 500e-6;       // Cantilever  Length
parameter real Wc = 100e-6;       // Cantilever  Width
parameter real Rf = 5;            // Coil  resistance
parameter real Rj = 1e3;          // Gauge nominal resistance
parameter real Tgf = 32;          // (DR/R) in  1/Newton unit

// Nodes declaration
real            DRj;
kinematic       FORCE_EXT;
kinematic       BEND;
kinematic_v     VELOCITY;

// Behavior description
analog
      begin

      // Ohm's law in the actuating coil
      V(fa, fb) <+ Rf * I(fa, fb);

      // Lorentz Force
      F(FORCE_EXT) <+ I(fa,fb) * Wc * T(B);

      // Mechanical Noise Power Spectral Density
      F(FORCE_EXT) <+ white_noise ( 4 * 1.38e-23 * 300 * D );

      // Differential equation set
      Vel(VELOCITY) <+ ddt(Pos(BEND));
      Pos(BEND) <+   (1/K)*F(FORCE_EXT);
      Pos(BEND) <+ - (D/K)*Vel(VELOCITY);
      Pos(BEND) <+ - (M/K)*ddt(Vel(VELOCITY));

      // Change in gauge resistance
      DRj = Rj * Tgf * (Lc/Wc) * K * Pos(BEND);

      // Ohm's law in the gauge
      V(ra, rb) <+ (Rj + DRj) * I(ra, rb);

      // Johnson Noise in the Gauge
      V(ra, rb) <+ white_noise ( 4 * 1.38e-23 * 300 * Rj );

      // Outputs bending for debug
      Pos(z) <+ Pos(BEND);

      end
endmodule
```

Figure 6: Behavioral HDL description of the filter.

3 SYSTEM-LEVEL SIMULATIONS

The simulation of such an heterogeneous system faces several difficulties: (i) it combines mechanical and electronic parts, (ii) the high-Q mechanical device exhibits large time constant in comparison with oscillations period leading to time-consuming transient simulations before a steady state is achieved and (iii) the frequency translation introduced by the mixer requires specific tools for small-signal analysis. For this particular application, the proposed design methodology relies on the use of standard microelectronic CAD tools, in our case the Cadence® design framework and Spectre-RF® simulation engine.

Although sounding like an RF extension of the traditional SPICE-like simulator, Spectre-RF® has been designed to handle any periodically time-varying systems such as mixers or switched-capacitors filters regardless their operating frequencies [4]. The simulator comes with an analysis suite including PSS (Periodic Steady State), which can speed up the steady-state calculation for systems having large settling times, PAC (Periodic AC), PXF (Periodic Transfer Function) and PNOISE (Periodic Noise Analysis) that perform small-signal analysis based on a periodically time-varying operating point.

3.1 The test bench

The purpose of the proposed simulation is to verify the system ability to measure the frequency compounds of a *50Hz* square. The square signal is then applied to the V_{meas} input of the circuit whereas V_{fs} receive a frequency sweep (ac) stimuli.

In order to interpret the simulation results, one should remember that the successive harmonics of a square wave *S* of amplitude *1* is given by the Fourier transform:

$$S(t) = \frac{4}{\pi}\sum_{n=0}^{n=\infty}\frac{(-1)^n}{2n+1}\cos\left[2.\pi.(2n+1)f_{fund}.t\right] \qquad (3)$$

With *n*, the harmonic index. In our case, *n=1* corresponds to the third-order harmonic at *150Hz*, which amplitude represents *1/3* of the fundamental amplitude *(-10dB)*. The next frequency compound is the fifth-order harmonic (*n=2*) which amplitude is *1/5* of the fundamental amplitude (*-14dB*).

3.2 Periodic Steady-State Analysis

The Periodic Steady State (PSS) analysis is a large signal analysis that directly computes the periodic response of the circuit, with a simulation time being independent of the time constant of the circuit. The fundamental period for a PSS analysis has to be selected as an integral multiple of the period of each built-in time-varying independent source in the circuit. Due to the *50Hz* input on V_{meas}, a *20ms* PSS period is then chosen for our system.

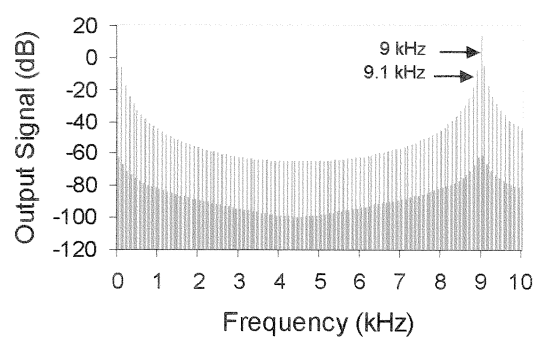

Figure 7: Result of the PSS analysis.

The PSS analysis computes the system steady state in both time and frequency domains. For example, the spectrum of the system output signal presented on figure 7 has been obtained using a single frequency signal of

9.05kHz on V_{fs}. Using such inputs, first order sidebands are located at *9kHz* and *9.1kHz*. As a result of the selective cantilever filtering, the *9.1kHz* tone is about *-25dB* below the *9kHz* tone. This result was expected due to the filter high selectivity.

3.3 Periodic AC Analysis

The periodic AC (PAC) analysis allows for computing transfer functions that include frequency translation, which is the case of our example. This analysis applies a small ac signal at the mixer input V_{fs} while the system is periodically varying at the *50Hz* frequency, as a result of the square signal on the V_{meas} input. Transfer functions (similar to standard AC analysis) are then computed then for each harmonic of the *50Hz* signal.

In the result presented on figure 8, the x-axis represents the system output frequencies responding to a narrow frequency sweep from *8.8kHz* to *9.2kHz* on V_{fs}. Note that a broader frequency sweep has been used to verify that the system output signal only features a *9kHz* single tone, resulting from the mechanical filtering. It appears that the system response is maximal for the fundamental *50Hz* tone. Next, come the third order harmonic (*150Hz*) and the fifth order harmonic (*250Hz*). This result was obviously expected since the square signal V_{meas} only contains odd order harmonics. Obtained amplitudes also comply with the Fourier transform results. The simulation has been restricted to five harmonic orders to limit the simulation time to few minutes.

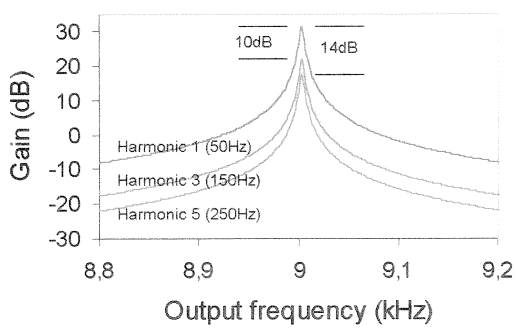

Figure 8: Result of PAC analysis (x-axis = "out")

Figure 9 displays the result of a similar PAC analysis, viewed from the input signal side. Here, the specified frequency range has been set from *8.5kHz* to *9.5kHz*. The obtained curves are interpreted as follow: input frequencies of V_{fs} at *8,95kHz* and *9.05kHz* produce the maximum output signal when mixed together with the V_{meas} fundamental *50Hz* tone (harmonic 1 and harmonic –1). Other peaks are found every time the sum (or the difference) of V_{fs} frequency and the square wave frequency compounds equals *9kHz*. Peaks at *8.85kHz* and *9.15kHz* then correspond to the third order *150Hz* harmonic of the V_{meas} signal, and so on.

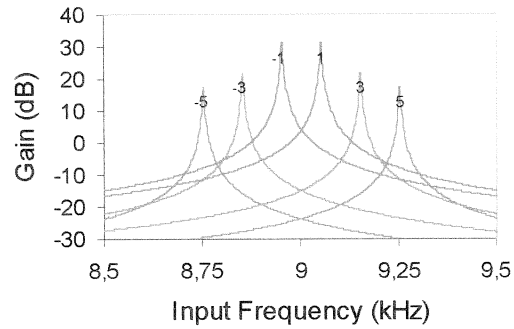

Figure 9: Result of PAC analysis (x-axis = "in").

Finally, the shape of the transient output signal envelope in response to a frequency sweep may be computed by summing the contribution of the square wave harmonics as shown figure 10. It verifies that the proposed system performs the required spectrum analysis. The recovery of the square wave spectrum only requires shifting down the so-obtained spectrum by a frequency amount that corresponds to the filter central frequency (*9kHz* here).

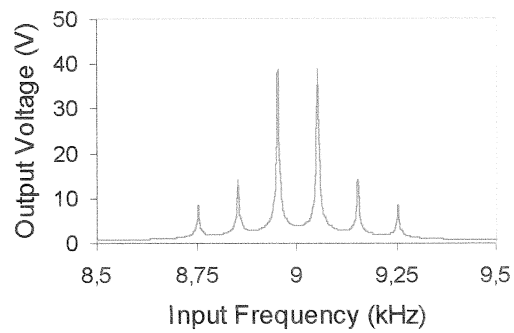

Figure 10: Sum of all harmonics contribution.

4 CONCLUSION

The study presented in this paper demonstrated the efficiency of electrical simulators in the design of a MEMS based system. Based on an extensively studied cantilever device, a mechanical filter has been implemented and integrated into the standard microelectronic design flow. With a spectrum analyzer application, several simulation difficulties such as long settling time and frequency translation have been solved using recent advances in the RF simulation field.

REFERENCES

[1] H. Baltes et al, "CMOS MEMS – Present and Future", IEEE MEMS, Las-Vegas (NV), USA, January 20-24, 2002, pp.459-466

[2] IEEE Standard for spectrum analyzers, IEEE Std 748-1979

[3] L. Latorre and al., "Characterization and modeling of a CMOS-compatible MEMS technology", Sensors and Actuators, Vol. 74, 1999, pp. 143-147

[4] Cadence SpectreRF® Tools, Lecture Manual, Version 4.4.6.,October, 2001.